

PHOTOLUMINESCENCE AND TEMPERATURE-DEPENDENT EMISSION STUDIES OF Au₂₅ CLUSTERS IN THE SOLID STATE

EDAKKATTUPARAMBIL S. SHIBU* and THALAPPIL PRADEEP†

DST Unit on Nanoscience (DST UNS)

*Department of Chemistry and Sophisticated Analytical Instrument Facility
Indian Institute of Technology, Madras, Chennai 600 036, India*

**shibuchem@gmail.com*

†pradeep@iitm.ac.in

Effect of ligand exchange on the optical and photoluminescence properties of Au₂₅SG₁₈ (SG-glutathione thiolate) clusters was investigated. A fluorescein-based dye, 5-((2-(and-3)-S-(acetylmercapto)succinoyl)amino)-fluorescein (SAMSA) was anchored on water soluble Au₂₅SG₁₈ clusters by the place exchange reaction and the solid-state emission of the exchange product was studied. Inherent fluorescence image of these clusters was mapped. Organic soluble Au₂₅(SC₂H₄Ph)₁₈ clusters were synthesized as a model system which also showed temperature-dependent solid-state emission, in good agreement with the results from water soluble Au₂₅ clusters.

Keywords: Au₂₅; Raman spectroscopy; solid-state emission; metal clusters.

1. Introduction

Monolayer-protected clusters (MPCs), especially subnanometer regime nanoparticles gained attention in various fields of science and technology due to their unusual optical,¹ electronic,² and catalytic³ properties which offer opportunities to study size-dependent evolution of phenomena. Gold nanoclusters are a new class of materials made up of tens to hundreds of atoms having intermediate composition between bulk and molecular regimes, where the electronic structure is molecule-like. Nanoclusters with diameters of 1–2 nm show discrete electronic transitions among the quantized levels and can be used in catalysis,⁴ nanoelectronics⁵ and sensing applications.⁶ Syntheses of Au₁₁,⁷ Au₅₅,⁸ and Au₈ are significant developments in cluster science. Several of these molecular clusters are fluorescent; for example, Au₈ nanodots encapsulated in PAMAM (G2-OH and G4-OH)

dendrimers exhibit a fluorescence quantum yield of 41%, more than 100-fold enhancement over other reported gold nanoclusters.⁹ In addition to Au₈, other clusters such as Au₅, Au₁₃, Au₂₃, and Au₃₁, were also encapsulated in the PAMAM cavity and they exhibit discrete excitation and emission spectra from the ultraviolet to near infrared region.¹⁰ Thiolate-protected gold (Au_n:SG_m) clusters with core containing less than 100 atoms have considerable interest because they show unique properties due to their molecule-like electronic transitions. First attempt to make glutathione protected nanoclusters was by Whetten and co-workers.^{11,12} Mass spectrometry confirmed that Au₂₈(SG)₁₆ was the most abundant species in this synthesis. Recently, a series of glutathione thiolate (SG-thiolate) protected gold clusters with well-defined compositions were synthesized.¹³ The different fractions were separated utilizing polyacrylamide gel

electrophoresis (PAGE).^{13,14} The molecular compositions of these clusters were characterized by electrospray ionization (ESI) mass spectrometry. Chemical etching reaction of these clusters with excess glutathione was used to synthesize Au₂₅SG₁₈ in gram scale.¹⁵ The crystal structure of Au₂₅SG₁₈ was solved recently.¹⁶ The photophysical properties of these clusters could be tuned by the incorporation of desired molecules.

Herein, we report the functionalization of water soluble Au₂₅ clusters with a fluorescein-based dye known as SAMSA by the place exchange reaction. Presence of SAMSA on Au₂₅ clusters was ensured by UV-Vis spectroscopy. The solid-state emission and inherent fluorescence images of Au₂₅-SAMSA were also measured by using a confocal Raman microscope. Temperature-dependent solid-state emission of Au₂₅(SC₂H₄Ph)₁₈ was also studied, which is in good agreement with water soluble Au₂₅ clusters.¹⁷ The acronym Au₂₅-SAMSA refers to Au₂₅ clusters functionalized with SAMSA.

2. Experimental Details

All the chemicals were commercially available and were used without further purification. HAuCl₄ · 3H₂O, methanol (GR grade) and ethanol (GR grade) were purchased from SRL Chemical Co. Ltd, India. NaBH₄ (> 90%), GSH (γ -Glu-Cys-Gly), tetraoctylammonium bromide (TOAB) and phenyl ethane thiol (PhC₂H₄SH) were purchased from Sigma Aldrich. SAMSA was purchased from molecular probes. SAMSA was activated by using a reported procedure.¹⁸

2.1. Synthesis of Au@SG

Au@SG nanoparticles were synthesized using a reported procedure.¹⁴

2.2. Synthesis of Au₂₅SG₁₈ from crude Au@SG

Au₂₅SG₁₈ clusters were synthesized using a reported protocol.¹⁵

2.3. Exchange reaction with SAMSA

About 20 mg of Au₂₅SG₁₈ was dissolved in 5 mL of SAMSA solution (2 mg/mL) and stirred for 3 h

at room temperature. The exchange product was precipitated using methanol and centrifuged at 20 000 rpm for 30 min. The exchange product was washed three times with ethanol and dried to yield a black brown powder.

2.4. Synthesis of Au₂₅(SC₂H₄Ph)₁₈

Au₂₅(SC₂H₄Ph)₁₈ was synthesized using a reported procedure.¹⁶

3. Instrumentation

UV-Vis spectra were recorded using a Perkin Elmer *Lambda 25* spectrometer. The Raman and fluorescence images were measured by using a Witec GmbH confocal Raman spectrometer equipped with a 514.5 nm Ar ion laser with a spot size < 1 μ m. Temperature-dependent fluorescence data were collected with an Oxford cryostat mounted on the Raman spectrometer and lower temperatures were obtained by liquid nitrogen circulation.

4. Results and Discussion

Figure 1 shows the UV-Vis spectra of Au₂₅SG₁₈, SAMSA, and Au₂₅-SAMSA. The concentration of SAMSA and Au₂₅SG₁₈ used for UV-Vis measurements was $\sim 10^{-6}$ and 10^{-4} M, respectively. Inset shows the corresponding energy profile diagram of parent Au₂₅ clusters, showing all the possible electronic transitions. Three distinct electronic transitions are possible and it is shown by a-c.²⁰ Here, a represents the HOMO-LUMO transition and b and c represent the HOMO-sp and d-sp transitions, respectively. SAMSA shows an absorption peak

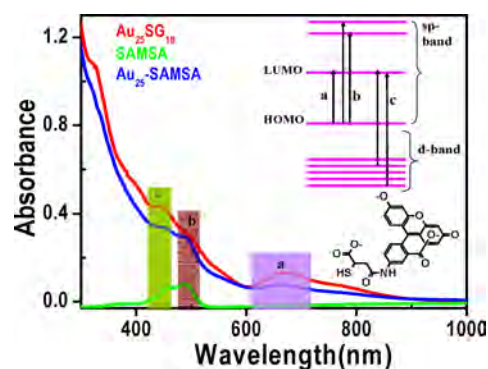


Fig. 1. UV-Vis spectra of Au₂₅SG₁₈, SAMSA, and Au₂₅-SAMSA in water. Inset shows the corresponding energy profile diagram of parent Au₂₅ cluster showing all the possible transitions (a-c). Molecular structure of SAMSA is also given.

at 498 nm. The same absorption peak was observed in the exchanged product also. Even though this peak is merged with b, we could see the distinct hump in the corresponding region. Both parent and exchanged clusters have all the three transitions. This clearly shows that after the exchange reaction there is no change in the core size of the cluster. Intra-band transition of parent cluster comes around 672 nm, which is in good agreement with the other Au₂₅ clusters reported so far.^{14–17,19} In the case of Au₂₅-SAMSA, the intra-band transition shows a blue shift of 5 nm and it could be due to the strong electronic interaction between the π electron cloud of SAMSA ring with the Au₂₅ core.

We studied the solid-state emission of Au₂₅-SAMSA. A 1×10^{-3} M solution of Au₂₅-SAMSA was prepared in water and it was drop casted on a thin glass plate and dried at room temperature. Figure 2(a) shows the solid-state emission collected from SAMSA and Au₂₅-SAMSA. The emission maximum comes around 725 nm, a red shift of 25 nm compared to the parent Au₂₅ clusters. The red shift could be attributed to the strong electronic interaction between the SAMSA and Au₂₅ core in the solid state. This type of interaction between SAMSA and gold nanoparticles is known in the solid-state.¹⁸ In addition to the emission at 725 nm, a new emission peak comes around 550 nm. This could be from the SAMSA molecule sitting on Au₂₅. Figure 2(b) shows the inherent fluorescent image ($10 \mu\text{m} \times 10 \mu\text{m}$) of Au₂₅-SAMSA collected using the emission peak at 725 nm. Solid-state emission from Au₂₅SG₁₈ clusters has been reported before.¹⁷ This compound did not show any Raman features. It appears that Raman features were merged in the inherent fluorescence as the latter is much more intense. SAMSA is a fluorescein-based dye with an

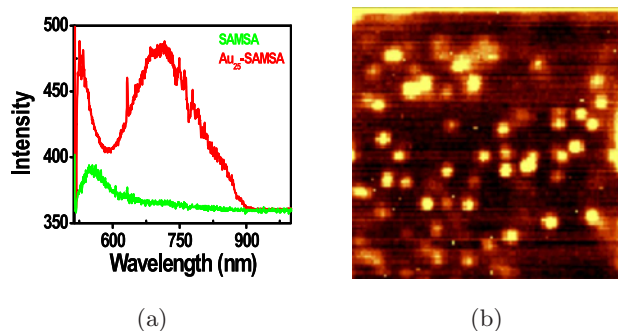


Fig. 2. (a) Solid-state emission from SAMSA and Au₂₅-SAMSA. (b) Inherent fluorescence image collected by the spectroscopic mapping of an area of $10 \mu\text{m} \times 10 \mu\text{m}$.

aromatic ring. In the solution state, the SAMSA will interact with gold clusters but the extent of interaction is very small due to less number of fluorophores per cluster. In solid-state, both dye and gold core come close to each other. This will lead the efficient interaction of gold clusters with the fluorophores.

We synthesized organic soluble Au₂₅ clusters and characterized using UV-Vis spectroscopy. Figure 3 shows the UV-Vis spectra of Au₂₅(SC₂H₂Ph)₁₈ (in acetonitrile, 10^{-4} M) and Au₂₅SG₁₈ (water, 10^{-4} M). Organic Au₂₅ clusters also show three distinct transitions and peak positions are matching exactly with those of water soluble Au₂₅ clusters. In both cases, the intra-band transition comes around 672 nm. Inset shows an expanded view of the intra-band transition. Schematic of the corresponding clusters is also given.

We studied the temperature dependence on the solid-state emission of organic Au₂₅ and it was compared with water soluble Au₂₅ clusters (Fig. 4(b)).¹⁷ Experiment was carried out at various temperatures from 80 K to 300 K at an interval of 10 K. At 80 K the emission intensity was very small and gradually increased with increasing temperature. But up to 160 K, the increment in intensity was small and pronounced enhancement was observed only after 160 K. The emission occurs at the same position throughout the temperature window indicating that there are no geometric changes in the system affecting its electronic structure. Coming to the decrease

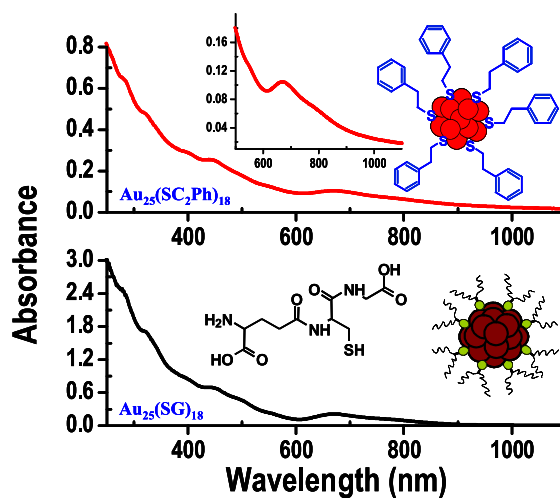


Fig. 3. UV-Vis spectra of Au₂₅(SC₂H₄Ph)₁₈ and Au₂₅SG₁₈ in acetonitrile and water, respectively. Inset shows an expanded region of intra-band transition of organic Au₂₅ clusters. Note that intra-band transition comes at 672 nm in both the cases. Molecular structure of glutathione and schematic of the two clusters are also given.

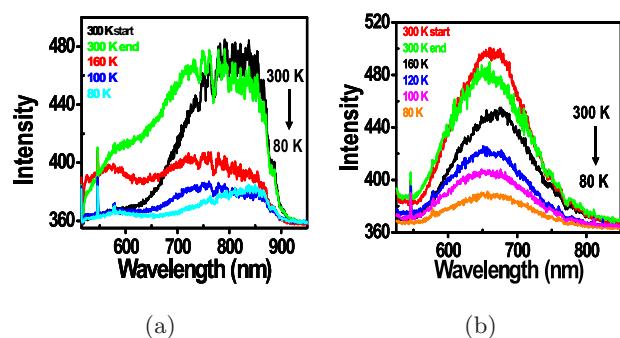


Fig. 4. (a and b) Temperature-dependent solid-state emission from $\text{Au}_{25}(\text{SC}_2\text{H}_4\text{Ph})_{18}$ and $\text{Au}_{25}\text{SG}_{18}$. Note that the emission retained its intensity in both cases even after a complete cycle of the experiment.

in the intensity of the fluorescence with decreasing temperature, the non-radiative relaxation channel becomes prominent with decrease in temperature. Although no explanation can be proposed, it suggests significant vibrational relaxation. However, no transition was detected in differential scanning calorimetry down to 173 K.

5. Conclusion

Ligand exchange reaction on Au_{25} was performed using a fluorescein-based dye, SAMSA. Solid-state emission of the exchange product was studied. This intense emission allows the optical imaging of the materials in the solid-state. Organic soluble $\text{Au}_{25}(\text{SC}_2\text{H}_4\text{Ph})_{18}$ clusters were synthesized as a model system and their temperature-dependent solid-state emission was studied in the 300–380 K window, in good agreement with water soluble $\text{Au}_{25}\text{SG}_{18}$ clusters. Solid-state emission from these clusters was found to be temperature-dependent and suggests hardening of phonons with decrease in temperature.

Acknowledgments

The authors thank the Department of Science and Technology (DST), Government of India for constantly supporting our research program on nano-materials. E. S. S. thanks the University Grants Commission (UGC) for a senior research fellowship.

References

1. W. P. Wuelfing, S. J. Green, J. J. Pietron, D. E. Clif-fel and R. W. Murray, *J. Am. Chem. Soc.* **122**, 46 (2000).
2. P. Schwerdtfeger, *Angew. Chem. Int. Ed.* **42**, 1892 (2003).
3. H. Tsunoyama and T. Tsukuda, *J. Am. Chem. Soc.* **127**, 9364 (2005).
4. H. Tsunoyama and T. Tsukuda, *Langmuir* **20**, 11293 (2004).
5. S. Chen, R. S. Ingram, M. J. Hostetler, J. J. Pietron, R. W. Murray, T. G. Schaaff, J. T. Khoury, M. M. Alvarez and R. L. Whetten, *Science* **280**, 2098 (1998).
6. T. Huang and R. W. Murray, *J. Phys. Chem. B* **105**, 12498 (2001).
7. P. A. Bartlett, B. Bauer and S. Singer, *J. Am. Chem. Soc.* **100**, 5085 (1978).
8. G. Schmis, R. Boese, B. Pfeil, F. Andermann, S. Meyer, G. H. M. Calis and J. W. A. Van der Velden, *Chem. Ber.* **114**, 3634 (1981).
9. J. Zheng, J. T. Petty and R. M. Dickson, *J. Am. Chem. Soc.* **125**, 7780 (2003).
10. J. Zheng, C. W. Zhang and R. M. Dickson, *Phys. Rev. Lett.* **93**, 077402 (2004).
11. T. G. Schaaff, G. Knight, M. N. Shafiqullin, R. F. Borkman and R. L. Whetten, *J. Phys. Chem. B* **102**, 10643 (1998).
12. T. G. Schaaff and R. L. Whetten, *J. Phys. Chem. B* **104**, 2630 (2000).
13. Y. Negishi, K. Nobusada and T. Tsukuda, *J. Am. Chem. Soc.* **127**, 5261 (2005).
14. Y. Shichibu, Y. Negishi, T. Tsukuda and T. Teranishi, *J. Am. Chem. Soc.* **127**, 13464 (2005).
15. Y. Shichibu, Y. Negishi, H. Tsunoyama, M. Kanehara, T. Teranishi and T. Tsukuda, *Small* **3**, 835 (2007).
16. M. W. Heaven, A. Dass, P. S. White, K. M. Holt and R. W. Murray, *J. Am. Chem. Soc.* **130**, 3754 (2008).
17. E. S. Shibu, M. A. H. Muhammed, T. Tsukuda and T. Pradeep, *J. Phys. Chem. C* **112**, 12168 (2008).
18. N. Nishida, E. S. Shibu, H. Yao, T. Oonishi, K. Kimura and T. Pradeep, *Adv. Mater.* **20**, 4719 (2008).
19. M. A. H. Muhammed, A. K. Shaw, S. K. Pal and T. Pradeep, *J. Phys. Chem. C* **112**, 14324 (2008).
20. M. Zhu, C. M. Aikens, F. J. Hollander, G. C. Schatz and R. Jin, *J. Am. Chem. Soc.* **130**, 5883 (2008).